



HAL
open science

The Linear Motor in the Human Neutrophil Migration

V. Vereycken, H. Gruler, C. Bucherer, C. Lacombe, J. Lelièvre

► **To cite this version:**

V. Vereycken, H. Gruler, C. Bucherer, C. Lacombe, J. Lelièvre. The Linear Motor in the Human Neutrophil Migration. *Journal de Physique III*, 1995, 5 (9), pp.1469-1480. 10.1051/jp3:1995204 . jpa-00249395

HAL Id: jpa-00249395

<https://hal.science/jpa-00249395v1>

Submitted on 4 Feb 2008

HAL is a multi-disciplinary open access archive for the deposit and dissemination of scientific research documents, whether they are published or not. The documents may come from teaching and research institutions in France or abroad, or from public or private research centers.

L'archive ouverte pluridisciplinaire **HAL**, est destinée au dépôt et à la diffusion de documents scientifiques de niveau recherche, publiés ou non, émanant des établissements d'enseignement et de recherche français ou étrangers, des laboratoires publics ou privés.

Classification
Physics Abstracts
87.25 — 87.45

The Linear Motor in the Human Neutrophil Migration

V. Vereycken⁽¹⁾, H. Gruler⁽²⁾, C. Bucherer⁽¹⁾, C. Lacombe⁽¹⁾ and J.C. Lelièvre⁽¹⁾

⁽¹⁾ Unité de Biorhéologie, Université Paris VI et CNRS LBHP URA 343 CHU Pitié-Salpêtrière, 91 bd de l'Hôpital, 75013 Paris, France

⁽²⁾ Chaire scientifique Roger Seydoux de la Fondation de France, Centre d'Ecologie Cellulaire, Groupe Hospitalier Pitié-Salpêtrière, 75651 Paris Cedex 13, France
Abteilung Biophysik Universität Ulm, 89069 Ulm, Germany

(Received 13 February 1995, revised 11 May 1995, accepted 25 May 1995)

Abstract. — The kinematics and dynamics of human neutrophils in a narrow glass tube ($4.9 \mu\text{m}$ to $6.3 \mu\text{m}$ in diameter) have been investigated both experimentally and theoretically. Cells were activated by the tri-peptide (fMLP) to migrate through a tube with a mean speed of $0.15 \pm 0.03 \mu\text{m/s}$ (54 activated cells). When a hydrostatic pressure was applied across the cell, the mean speed of the cell leading front linearly decreases when the pressure is increased. At a pressure difference of $1530 \pm 140 \text{ Pa}$ (9 activated cells), the cell was forced to stop. The cell migration has been approximated by a tractor-trailer model. The cellular motor (leading front), the tractor, produced a traction force by converting chemical energy into mechanical work. This motor has been characterized as a linear motor with two machine coefficients: (i) the maximum traction T_0 (37.7 nN) at $V = 0$, where V is the cellular speed (ii) the maximum cellular speed V_{max} ($0.15 \mu\text{m/s}$). A characteristic time of approximately 100 s was measured for the action cycle of the linear motor. A phenomenological description of the chemotactic machine has been presented.

1. Introduction

Cells like leucocytes, fibroblasts, neural crest cells, etc., can adhere on a substrate in order to move and they have the ability to respond to extracellular chemical and physical signals resulting in directed and non-directed movement [1]. These cell types migrate like an amoeba by continuously changing their shape. It is the aim of this paper to investigate the motile machinery which governs these kinds of motion. Our investigations are performed on human neutrophils which form the first defense line against invading microorganisms.

The cellular automatic controller responsible for directed and non-directed movement is investigated in an experimental set-up where the cells have the possibility to migrate on a plane surface [2]. However, if the cells are forced to migrate in a narrow tube ($D > 2R$, where D is the characteristic length of the cell and R the radius of the tube) as first described by Usami *et al.* [3], then the cell direction of migration is determined by the glass tube (Fig. 1).

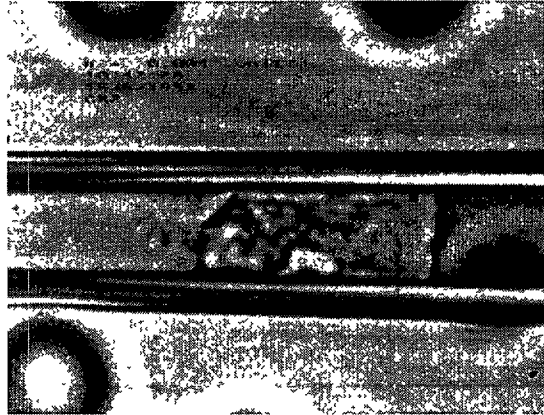


Fig. 1. — Micrograph of a human neutrophil stimulated by a chemoattractant to migrate in a glass tube. The leading front on the right and the cell body on the left can be easily distinguished. The pipette diameter is $5.17 \mu\text{m}$. The measured mean speed of the cell is $0.14 \mu\text{m/s}$.

If the basic biochemical reactions of the cellular signal transduction chain begin to be studied and interpreted, the related physical events are much less understood. In addition to the main function of separating the intracellular space from the extracellular one, the membrane is the first element involved in the signal transduction chain which can be described as follows.

Detection system: specific molecules stimulating chemokinesis and chemotaxis bind to the cell membrane receptors and create the primary intracellular signal.

Amplification chain: the activated receptors are the first elements involved in the biochemical amplification chain. One loaded receptor activates many membrane-attached G-proteins. The G-protein activates the phospholipase-C. One phospholipase-C molecule hydrolyses many ATP-activated phospholipid (phosphatidylinositol) molecules at the inner side of the membrane. The water soluble head group inositol triphosphate opens calcium channels and intracellular calcium stores. Inositol triphosphate and calcium are regarded as secondary cellular messengers.

Motor: Stossel [4] suggests that the increased intracellular calcium concentration is responsible for the cytoskeleton contraction but the function of the repetitive increases in calcium remain unsolved [5]. However, controversial results show that (i) calcium alone cannot play a prominent role in the cell shape control [6] (ii) calcium rise triggered by fMLP is not essential for the extensive morphological changes usually observed.

2. Materials and Methods

Neutrophils are obtained from fresh blood samples by finger prick, and Heparin is used as anticoagulant. Neutrophils are diluted in Hanks Balanced Salt Solution (HBSS).

Glass tubing (Kwick-fill standard, Phymep, Paris, France, $1.20 \text{ mm O.D.} \times 0.69 \text{ mm I.D.} \times 15 \text{ cm}$ length, Clark Electromedical Instrument) is pulled with the aid of a vertical micropipette puller (Narishige, MO.202, Tokyo, Japan). The closed tip of the micropipette is snapped off with a microforge (De Fonbrune, Alcatel, Annecy, France) in order to obtain a flat tip and parallel side micropipette with an internal tip diameter between 4.9 and $6.3 \mu\text{m}$. Pipettes are filled with HBSS. The cells are stimulated to migrate by the tri-peptide fMLP (N-Formyl-

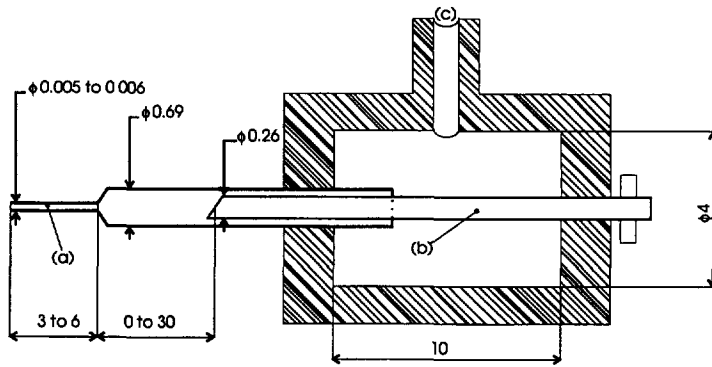


Fig. 2. — Schematic section of the glass micropipette in which the spontaneous cell movement can be observed. (All dimensions in mm). A microneedle b), 0.26 μm in inner diameter, filled with fMLP is inserted in the micropipette a), whose tip diameter is in the range of 4.9 μm and 6.3 μm . The chamber c) is connected to a pressure system which allows a counter pressure to be applied to the moving cell.

Methionyl-Leucyl-Phenylalanine) supplied by Sigma (Saint-Quentin Fallavier, France). Stock solutions are prepared with ethanol and stored at a concentration of 10^{-2} M between 0 and 4 °C. fMLP solutions are prepared at different concentrations (μM to nM).

A small needle (0.46 mm O.D. \times 0.26 mm I.D. \times 51 mm length), containing 9×10^{-7} M of f-Met-Leu-Phe, in 1% gelatin (Sigma), is inserted in the micropipette filled with HBSS (Fig. 2).

The micropipette is connected to a micromanipulator (Narishige) mounted on an inverted IMT2 microscope (Olympus, Optical Corp. Ltd, Tokyo, Japan). Pressure inside the micropipette can be adjusted by a pressure transducer (connected to the pipette).

Neutrophil suspension is injected into a glass microchamber (14 mm length, 10 mm width and 2.5 mm thick) and put on the microscope stage.

The tip of the micropipette is placed into the chamber close to a cell. It takes experimentally between 2 and 3 hours until the fMLP concentration is high enough at the tip of the micropipette for the neutrophil to register the chemoattractant compound, to direct its movement toward the tip of the micropipette and to migrate inside the micropipette. An example of the concentration profile of fMLP for a diffusion time of 2h47min has been computed [7] from the diffusion equations with the two diffusion coefficients of fMLP, 34.7×10^{-5} mm^2/s and 45.2×10^{-5} mm^2/s , respectively in gelatin and buffer [8]. The resulting diffusion profile is shown in Figure 3.

Neutrophils and their active movement are observed with the inverted microscope (Olympus, 40×1.5 , 60×1.5). Experiments are recorded on videotape (JVC, HR-D650MS, Victor Company of Japan, Ltd, Tokyo, Japan) with a camera (Cohu, Tokyo, Japan) for a delayed analysis. Time and pressure are displayed on the video monitor (Hitachi Denshi Ltd, Tokyo, Japan) with a data mixer (SOFRIG, Société Française d'Informatique et de Graphisme, Bobigny, France).

All experiments are performed at room temperature.

Next, the tractor-trailer model is discussed for a cell migrating in a tube.

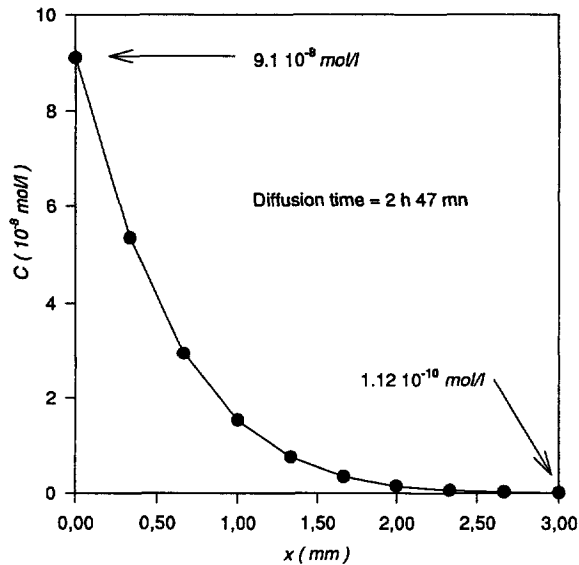


Fig. 3. — Example of fMLP concentration profile along the micropipette for an initial concentration of fMLP in the microneedle equals to $0.9 \mu\text{M}$ (see Fig. 2). At the micropipette tip, the fMLP concentration computed for a diffusion time of 2 h 47 mn and for the two diffusion coefficients of fMLP, $34.7 \times 10^{-5} \text{ mm}^2/\text{s}$ and $42.5 \times 10^{-5} \text{ mm}^2/\text{s}$ respectively in gelatin and in buffer, is $1.12 \times 10^{-10} \text{ mol/l}$. The computation of the concentration profile has been done by using a finite difference method which takes into account the overall diffusion process along the system represented in Figure 2.

3. The Tractor-Trailer Model

The motile machinery can be prepared out of a cell [9, 10]. A carefully controlled and timed application of heat causes the leading front of the cell to move forward rapidly, forming a long thin stalk between the actively moving cytokineplast and the remaining cell body. The newly formed cytokineplast is capable of directed and non-directed movement. The cytokineplast moves actively and drag the remaining part of the cell. Thus, the following model can be applied to a migrating cell: the leading front (cytokineplast) is the tractor and the remaining part of the cell is the trailer. This tractor-trailer model will be used to phenomenologically quantify the cellular migration.

A neutrophil adhering to a surface has the intrinsic possibility of motility. Exposure of the cell to a chemokinetic stimulus results in an active movement accompanied by characteristic cell shape and starting position changes. The contact area of the leading front and of the uropod (rear end) with the substrate are time dependent. A random movement is observed in case of a plane surface and an isotropic environment. However, in case of a narrow glass tube the cellular movement is restricted and, thus, easier to quantify: there is no change in the angle of migration and the morphological appearance of the leading front is rather stable in time. In addition, the strength of the cellular motor can be quantified if the cell has to migrate against a counter force due to a pressure difference. Thus, we have an ideal test system for investigating the amoeboid migration. In case of physical systems, the basic laws between

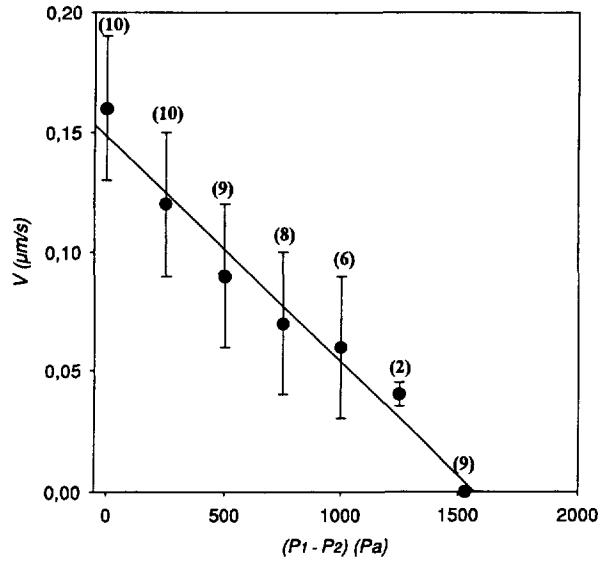


Fig. 4. — Mean speed V of a neutrophil in a micropipette (diameter $5.8 \pm 0.2 \mu\text{m}$) as a function of the pressure difference $(p_1 - p_2)$. The concentration of fMLP is $0.9 \mu\text{M}$ in the microneedle (see Fig. 2) and zero in the test chamber. The straight line is a linear regression which gives the two coefficients of the cellular machine. The numbers indicated in parenthesis correspond to the number of studied cells.

forces and movements are known. This concept will be applied to migrating cells.

The measured cellular speed linearly decreases when the pressure difference is increased (Fig. 4). The cell is forced to stop at the pressure difference $(p_1 - p_2)_0$. This pressure difference $(p_1 - p_2)_0$ equal to 1564 Pa is obtained by fitting a straight line to the measured data points (Fig. 4). The pressure difference $(p_1 - p_2)_0$ is experimentally found equal to $1530 \pm 140 \text{ Pa}$ ($n = 9$ cells).

Results of Figure 4 suggest to interpret the cell movement as a linear motor where the cell is the “rotor” and the pipette tube the “stator”. Let $T(V)$ be the traction undergone by the cell moving at the constant speed V . The force balance gives

$$T - F - C = 0 \quad (1)$$

where F is the friction force acting on the cell surface due to the pipette wall and C the load resulting from the pressure difference $(p_1 - p_2)$

$$C = \pi R^2 (p_1 - p_2) \quad (2)$$

Both F and C act in an opposite direction regarding to the traction T .

Assuming that the traction T is given by

$$T = T_0 \left(1 - \frac{V}{V_{\max}} \right) \quad T_0 \geq 0 \quad V_{\max} \geq 0 \quad (3)$$

where the two constants T_0 (the maximum traction) and V_{\max} (the maximum cellular speed) depend on the cellular machinery and probably also on the micropipette diameter. The

actin/myosin like microfilaments connected to the membrane are able to produce such a traction through bonds which link some part of the cell to the pipette wall.

A friction law has to be postulated for F , which may have one of the following simple forms

$$F = 0 \quad (4)$$

$$F = F_0 \quad (5)$$

$$F = kV \quad (6)$$

They correspond to the cases for which respectively (4) there is no friction between the cell surface and the pipette wall (5) one assumes a constant friction (6) the friction force is proportional to the cell speed. Either one of those cases leads to a linear relationship between the speed V and the motor load C as shown by the experimental results of Figure 4.

At this step, one can reasonably assume that there is no friction. For a non activated cell ($T_0 = 0$) aspirated in a micropipette, as long as a large fraction of the cell is outside the tube, the mean displacement of the cell is small due to the high intrinsic cell viscosity. However, no further cell shape changes are necessary when the cell is inside the tube and the cell moves very fast out of the viewing field. Thus, the friction between the cell body and the pipette wall can be neglected.

Thus using $F = 0$ and equations (1) and (3), it is easy to evaluate the linear motor constants T_0 and V_{\max} from the following equation:

$$\frac{V(C)}{V_{\max}} = 1 - \frac{C}{T_0} \quad (7)$$

with C given by equation (2). The constants can be obtained by fitting a straight line to the measured data points (Fig. 4). With a pipette diameter $2R_P$ of $5.6 \mu\text{m}$ and a pressure difference $(p_1 - p_2)_0$ of 1530 Pa the maximum traction T_0 is found to be equal to 37.7 nN and $V(C = 0) = V_{\max} = 0.15 \mu\text{m/s}$. These values T_0 and V_{\max} can be compared with our experimental values which are respectively $39 \pm 4 \text{ nN}$ and $0.15 \pm 0.03 \mu\text{m/s}$ and with those found by Usami *et al.* [3] which are respectively 30 nN and $0.33 \mu\text{m/s}$.

It is worthwhile to mention that the power P of the migrating neutrophil can be determined:

$$P = VT = VT_0 \left(1 - \frac{V}{V_{\max}} \right) \quad (8)$$

This power is zero for two cases: (i) for $V = 0$ (ii) for the maximum speed V_{\max} of the cell. For the later, the cell cannot perform additional work since the motor needs all its energy to overcome the internal friction originating from the steady reorganization of the cell motor. The cell can create its maximum power P_{\max} at half maximum speed

$$P_{\max} = \frac{T_0 V_{\max}}{4} \quad (9)$$

For $T_0 = 37.7 \text{ nN}$ and $V(C = 0) = 0.15 \mu\text{m/s}$ obtained from Figure 4, we find

$$P_{\max} = 1.4 \times 10^{-15} \text{ W} \quad (10)$$

The produced traction should be proportional to the contact area A_{motor} . In the case of a cylindrical leading front (cytokineplast) of Figure 5, the maximum tension $\sigma_0 = (T_0/A_{\text{motor}})$ can be determined: $\sigma_0 = 765 \text{ Pa}$ for a ratio R/L_0 approximately equals to 1 (Fig. 5). Considering the volume of the cytokineplast, this leads to the power density of 20.3 W/m^3 .

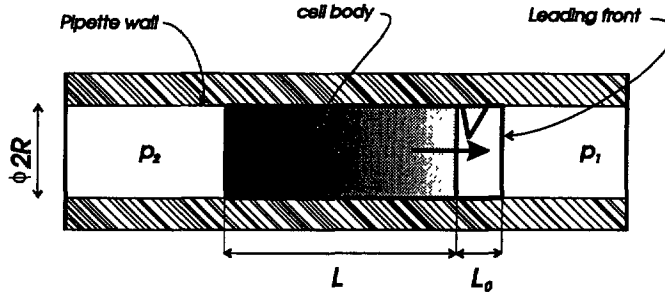


Fig. 5. — Schematic representation of a migrating cell at a mean speed V in a small tube of diameter $2R$. The leading front (clear zone) as the cellular motor is composed of an active surface element and has a well defined shape (cylinder of length L_0). The leading front produces the traction T which pulls the cell body (see text). The cell body is also cylindrically (length L) deformed by the tube. The friction force F (if it exists) produced by the gliding cell body, acts against the traction force of the motor (see text). A load C due to the pressure difference ($p_1 - p_2$) acts on the cell to slow down the cell speed.

The maximum tension σ_0 must be a function of the concentration c of the stimulating chemokinetic in the extracellular medium. The maximum tension applied to the cell should be proportional to the receptor occupancy. Thus we expect

$$\sigma_0 = \beta \frac{c}{c + K_R} \tag{11}$$

where K_R is the high affinity equilibrium binding constant of the chemokinetic to the receptor.

4. Phenomenological Model of the Signal Transduction Chain

Direct conversion of chemical into mechanical energy is one of the main processes in biological movements. Until now we have discussed the mechanical properties of the active surface element by two phenomenological coefficients T_0 and V_{\max} without taking into account any molecular events. Nothing has been said about the cellular machinery which is beyond the active surface element [10, 20].

An important result [11] is that the motile machinery of neutrophils (cytokineplasts) requires only a few elements: a part of the plasma membrane, microfilaments, unstructured cytoplasm as seen by light microscopy, and the required biochemistry.

Let us start with a phenomenological description of the cellular signal transduction chain. The simplified rate equation for the cellular second messengers, M , is:

$$\frac{dM}{dt} = k_t S - k_d M + \Gamma(t) \tag{12}$$

The first term describes the activation. The cell is stimulated by signal molecules like f-MLP to produce second messengers which, on the other hand, are responsible for the produced tension (traction). S is the primary cellular signal and k_t is a signal transduction coefficient [2, 12]. The second term describes the deactivation of the second messengers where k_d is a decay coefficient. The third term describes the stochastic processes in the signal transduction chain.

A general accepted picture is that the primary cellular signal, $S(c, t)$, is a function of the concentration c , of the signal molecules in the cellular environment and a function of time due to the temporal variation of the number of receptors. The model assumptions are: (i) the primary signal is proportional to the receptor occupancy [2, 12]

$$S(c, t) = R_0(t) \frac{c}{c + K_R} \quad (13)$$

where $R_0(t)$ is the total number of receptors exposed to the cell surface. (ii) The number of receptors is determined by machine cycles. For example: in the time interval $(0, t_1)$, R_0 receptors are exposed on the membrane and none receptor in the time interval (t_1, T) where T is the repetition time. The mean concentration of the second messenger, $\langle M \rangle$, can be obtained by solving [13] the differential equation (12) in the two time intervals.

$$\langle M \rangle = A \frac{c}{c + K_R} \quad (14)$$

A is approximately a constant in case of $k_d t_1 < 1$. The second messengers activate the active surface element and a tension is produced. It is assumed that the mean tension $\langle \sigma \rangle$ is proportional to the second messenger

$$\langle \sigma \rangle = K_A A \frac{c}{c + K_R} - K_D V \quad (15)$$

The construction of the surface active element becomes more difficult with increasing speed. Thus a second term is introduced. The mean cellular speed is

$$\langle V \rangle = A \frac{K_A}{K_D} \left(\frac{c}{c + K_R} \right) \quad (16)$$

if the friction of the cell body is neglected.

Now let us consider the concentration of the second messengers within one period of the machine cycle. As the receptor concentration, the second messenger concentration is expected to be time dependent. Consequently the cellular speed should show periodic fluctuation as actually observed when the movement of a cell in a narrow tube is investigated. The displacement of the cylindrical leading front as a function of time is shown Figure 6. The active migration is interrupted by resting states. This feature is clearly seen in time dependent speed (Fig. 6). A mean characteristic of the rythmic movement was estimated to 100 s by direct measurement in the graph of Figure 6.

The following experimental facts of the chemokinetic response are predicted by our model:

- the proportionality between mean cellular speed and high affinity receptor occupancy [2].
- The speed distribution induced by stochastic processes [2].
- The periodic fluctuation of the cellular speed.
- The speed dependent decrease in the lateral tension.
- The phenomenological model of the cellular signal transduction/response system is based on actual molecular events which will be discussed in the next section.

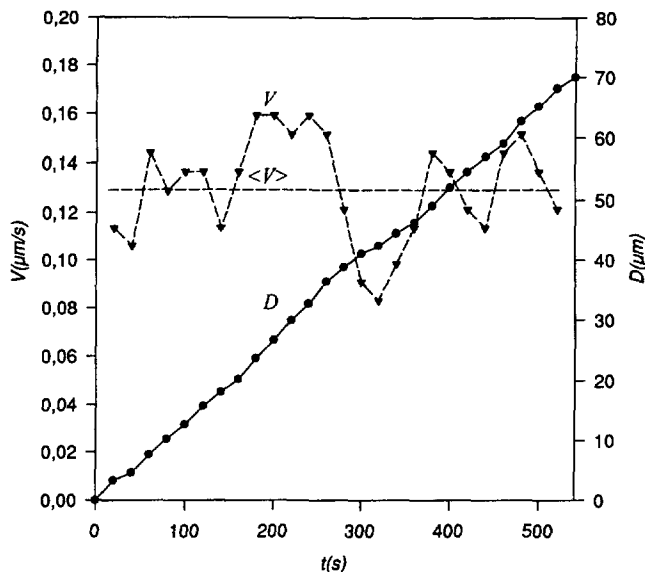


Fig. 6. — Displacement D and speed V of the front of the cell leading front as a function of time t . Mean speed $\langle V \rangle = 0.13 \mu\text{m/s}$. Pipette diameter $2R_P = 5.31 \mu\text{m}$. Cell diameter $2R_C = 8.23 \mu\text{m}$.

5. Molecular Aspects of the Motile Machinery

The cellular machinery needs in every machine cycle fresh receptors to communicate with its environment. We propose the following autocatalytic cycle. Step 1: intracellular second messengers like calcium or inositoltriphosphate, forces vesicles (loaded with fresh receptors) to fuse with the plasma membrane. Step 2: chemokinesis stimulating molecules bind to the new exposed receptors. Step 3: the activated receptors are the first elements in the biochemical amplification chain. One loaded receptor activates many membrane-attached G proteins. One G protein activates many phospholipase C molecules. One phospholipase C molecule hydrolyses many ATP-activated phospholipid (phosphatidylinositol) molecules at the inner side of the membrane. Step 4: the head group inositol triphosphate opens calcium channels and intracellular calcium stores and the remaining lipid diacylglycerol destabilizes the plasma membrane locally. Step 5: the increased intracellular second messengers concentration like calcium and inositoltriphosphate, triggers several cellular functions. First, the adhesion of the plasma membrane to the substrate must be time dependent and is likely controlled by the cellular second messengers. Second, the physical state of the microfilaments must also be time dependent and may be controlled by the second messengers. Third, the receptor molecules in the plasma membrane have to be renewed and this process may also be controlled by the second messengers. A new (measuring) cycle starts with the new receptors in the plasma membrane.

The first hint for the existence of a measuring cycle came from guiding field jump experiments. The first cellular reaction to a suddenly changed cellular environment (e.g., electric field, concentration gradient, etc.) was delayed by 8 to 10 s [14]. If such a measuring cycle exists in the cellular machinery then the cellular transfer function for migration should be frequency dependent with a characteristic time of 8-10 s. This was actually found when the cells were guided by pulsed electric fields. The measured cellular response was increased if the

repetition time of the pulses was manyfolds of 8 s. The measuring cycle of individual cells were synchronized by the pulsed electric guiding field [15]. In addition the electric potential difference across the plasma membrane should show periodic fluctuations with a characteristic time of ≈ 8 s as actually found [16].

There exists a further cycle in the cellular machinery for migration. The first hint came from the measured persistence time involved at random walk [13, 17, 18]. The measured time was approximately 60 s.

Both machine cycles (8 s and 60 s) do not seem to be related to the kinetics of receptor turnover which has been evaluated to be between 10 to 12 min [19].

It is a real machine cycle since the speed of migrating cytotineplasts periodically fluctuates with a characteristic time of ≈ 60 s [20]. In addition the electric potential difference [16] across the plasma membrane and the intracellular calcium concentration exhibit periodic fluctuations with a characteristic time of ≈ 60 s. The nature of this action cycle has not been yet evaluated. Our working hypothesis is that the cell communicates every 8 s with its environment, the received signals are integrated and the cell reacts every minute.

In the first stage of the machine cycle (100 s), the cell extends the lamellipod in the direction of movement. Adhesion receptors bind reversible with ligands attached to the underlying substratum. The cytoskeleton of the cell contracts during the second part of the cycle. If an asymmetric distribution of bonds is present, then there exists a net lateral tension (traction) and the cell experiences a net displacement. In the last stage of the cycle the cytoskeleton relaxes.

Cell adhesion is primarily mediated by surface receptors known as integrins (heterodimers composed of two subunits [21–23]). These integrins reversibly bind to extracellular matrix proteins like fibronectin and laminin [24]. The effect of variations of cell-substratum adhesiveness on the cell speed is mediated by the reversible integrin interaction with immobilized substrate ligands [25]. On poorly adhesive surface a cell may stick so weakly that no traction is obtained and no net movement occurs. Alternatively, a cell may attached to a highly adhesive surface so strongly that it becomes immobilized [26]. The necessary asymmetric distribution of adhesion proteins can be explained by the likely assumption that the fresh adhesion receptors are only supplied to the membrane at the front part of the cell [25].

A general accepted working hypothesis is that stored chemical energy of adenositriphosphate (ATP) is converted into mechanical work by means of microfilament proteins like actin and myosin which are enriched in the leading front. The principal protein for contraction is actin. 10% of the neutrophil protein is actin. Actin exposed to low salt concentrations depolymerizes to monomeric G-actin. In the presence of high enough ion concentrations the monomeric G-actin polymerizes to F-actin, a double helical polymer fiber with a typical length of 1 μm . Actin can also exist as a gel due to an actin binding protein which cross-links actin filaments. 1% of the neutrophil protein is actin-binding protein. This actin binding protein is a dimer and is composed of two highly flexible chains. Reversible crosslinking of actin fibers causes sol-gel transformation without any marked changes in the polymerized state of actin. Purified myosin in the presence of ATP contracts gels of actin and actin-binding protein. 1% of the neutrophil protein is myosin. Myosin is a hexamer composed of two polypeptide chains and four light chains. In summary, the actin network is essentially an electrically charged cross-linked polymer network within an ionic aqueous environment. We have a situation of fixed and movable charges, a problem known from semipermeable membranes. Actin Binding Proteins (ABP) play an important role as pointed out by Stossel [27]. Furthermore, the control of these proteins involves tyrosine phosphorylation and interactions with molecules such as PIP2. The state of actin is determined by intracellular ionic condition and the concentration and availability of proteins which bind actin. The physical properties of this polymer gel are

regulated by intracellular signals as calcium [28–30].

The elongation of the actin filaments at the leading edge is the first problem [31–33]. The basic event is that actin-profilin complexes diffuse to the plasma membrane where they are cleaved by the enzyme, E, to G-actin and profilin. The G-actin polymerizes onto the filament boundary close to the membrane. Thus, the polymerization of the filaments can be considered as a membrane controlled chemical reaction.

The contraction of the filament network can be discussed on the basis of polymer physics [34]. The gel is treated as a semi-dilute polymer solution (neglecting all the specific reactions) and the physical state of the gel is influenced by the cellular second messengers. The permeability of the gel in respect to the actin binding protein decreases with increasing concentration of the polymer binding proteins since the effective pore size becomes smaller. Two extreme cases of the machine cycle are of interest. At the moment of maximum stress the gel is attempted to contract. The polymer current is negative which means that polymer is flowing in and solvent is flowing out. At the moment of minimum stress the gel is attempting to expand. The polymer current is positive which means polymer is flowing out and solvent is flowing in.

The chemokinetic response can be summarized: the first cellular event in the machine cycle is the fusion of vesicles with the plasma membrane at the cellular front part. The vesicles contain (i) fresh receptors for binding the chemoattractant molecules of the extracellular space (ii) fresh adhesion proteins to maintain the asymmetric distribution of the cell adhesion (iii) lipids. The second cellular event is the start of the cellular amplification chain by the receptors loaded with specific molecules of the cellular environment. The result of this process is an altered concentration of second cellular messengers. A bifurcation takes place at this stage. (i) The second messengers can start again the machine cycle (self-ignition mechanism). (ii) The second messengers can influence the cross-linking of the polymer fibers and thus, the elastic tension of the polymer gel is altered. The periodic variations of the concentrations of the second messengers lead to periodic movements of the polymer gel. A rhythmic net displacement of the cell is obtained in case of a decreasing cell-substratum adhesiveness along the cell axis.

Acknowledgments

This work was supported in part by “Fond der Chemischen Industrie”, “Deutsche Forschungsgemeinschaft”, “Fondation de France”. We thank Y. Zerrouki who performed the finite difference computation of the f-Met-Leu-Phe concentration in the micropipette shown in Figure 3.

References

- [1] Trinkaus J.P., Cells into Organs (Prentice-Hall Inc., Engelwood Cliffs, New York, 1984).
- [2] Gruler H., in Lecture Notes in Biomathematics: Biological Motion, Alt W., Hofmann G., Eds (Springer Verlag, Heidelberg, 1990).
- [3] Usami S., Wung S., Skierczynski B., Skalak S. and Chien S., Locomotion forces generated by a polymorphonuclear leukocyte, *Biophys. J.* **63** (1992) 1663-1666.
- [4] Stossel T.P., The machinery of cell crawling, *Sci. Am.* (1994) 40-47.
- [5] Marks P.W. and Maxfield F.R., Transient increases in cytosolic free calcium appear to be required for the migration of adherent human neutrophils, *J. Cell Bio.* **110** (1990) 43-52.
- [6] Zaffran Y., Lepidi H., Benoliel A.M., Capo C. and Bongrand P., Role of calcium in the shape control of human granulocytes, *BLCED* **19** (1993) 115-131.
- [7] Dzisik M.N., Finite Difference Methods in Heat Transfer (CRC Press, NW, Bocaaton, Florida, USA, 1994).
- [8] Zicha D., Dunn G.A. and Brown A.F., A new direct-viewing chemotaxis chamber, *J. Cell Sci.* **99** (1991) 769-775.

- [9] Keller H.U. and Bessis M., Chemotaxis and phagocytosis fragments of human peripheral blood leukocytes, *Nouv. Rev. Fr. Hématol.* **15** (1975) 439-446.
- [10] Malavista S.E. and de Boisfleury-Chevance A., The cytokineplast: purified, stable and functional motile machinery from human blood polymorphonuclear leukocytes, *J. Cell Biol.* **95** (1982) 960-73.
- [11] Hallett M.B., Ed., *The Neutrophil : Cellular Biochemistry and Physiology* (CRC Press, inc, Boca Raton, Florida, USA, 1989).
- [12] Tranquillo R.T. and Lauffenburger D.A., Stochastic model of leukocyte chemosensory movement, *J. Math. Biol.* **25** (1987) 229-262.
- [13] Schienbein M., Franke K. and Gruler H., Random walk and directed movement: comparison between inert particles and self-organized molecular machines, *Phys. Rev. E* **49** (1994) 5462-5471.
- [14] Franke K. and Gruler H., Galvanotaxis of human granulocytes: electric field jump studies, *Eur. Biophys. J.* **18** (1990) 335-346.
- [15] Franke K. and Gruler H., Directed cell movement in pulsed electric fields, *Z. Naturforsch. Teil C.* **49** (1994) 241-249.
- [16] Jäger U., Gruler H. and Bültmann B., Morphological changes and membrane potential of human granulocytes under influence of chemotactic peptide and/or Echo-Virus, type 9, *Klin. Wochenschr.* **66** (1988) 434-436.
- [17] Peterson S.C. and Noble P.B., A two dimensional random-walk analysis of human granulocyte movement, *Biophys. J.* **12** (1972) 1048-1055.
- [18] Hall R.L. and Peterson S.C., Trajectories of human granulocytes, *Biophys. J.* **25** (1979) 365-372.
- [19] Niedel J.E. and Dolmatch B.L., Cellular processing of formyl peptide receptors, in *Leukocyte Locomotion and Chemotaxis*, (Keller H.U., Till G.O., Eds, Birkhäuser Verlag Basel, 1983) pp. 309-322.
- [20] Gruler H. and de Boisfleury-Chevance A., Chemokinesis and necrotaxis of human granulocytes: the important cellular organelles, *Z. Naturforsch. Teil C.* **42** (1987) 1126-1134.
- [21] Ruoslahti E., Integrins, *J. Clin. Invest.* **87** (1991) 1-5.
- [22] Springer T.A., Adhesion receptors of the immune system, *Nat.* **346** (1990) 425-34.
- [23] Larson R.S. and Springer T.A., Structure and function of leukocyte integrins, *Immunol. Rev.* **114** (1990) 181-216.
- [24] Ruoslahti E. and Pierschbacher M.D., New perspectives in cell adhesion, *Sci.* **238** (1987) 491-497.
- [25] Di Milla P.D., Barbee K. and Lauffenburger D.A., Mathematical model for the effects of adhesion and mechanics on cell migration speed, *Biophys. J.* **60** (1991) 15-37.
- [26] Lackie J.M. and Wilkinson P.C. *White Blood Cell Mechanics* (Lichtman M.A., La Celle P.C., Eds, A.R.Liss, New York, 1984).
- [27] Stossel T.P., How cells crawl, *Am. Sci.* **78** (1990) 408-423.
- [28] Boxer L.A. and Stossel T.P., Interactions of actin, myosin, and an actin-binding protein of chronic myelogenous leukemia leukocytes, *J. Clin. Invest.* **57** (1976) 964-976.
- [29] Stossel T.P., *Leukocyte chemotaxis: Methods, Physiology and Clinical Implications* (Gallin J.I. and Quin P.G., Eds, Raven Press, New York 1978).
- [30] Stossel T.P., Hartwig J.H., Yin J.L. and Stendahl D., The motor of amoeboid leukocytes, *Biochem. Soc. Symp.* **45** (1980) 651.
- [31] Oster G.F., Perelson A.S. and Tilney L.G., A mechanical model for elongation of the acrosomal process in tyrene sperm, *J. Math. Biol.* **15** (1982) 259-265.
- [32] Oster G.F., On the crawling of cells, *J. Embryol. exp. Morphol.* **83** (1984) 329-364.
- [33] Oster G.F. and Perelson A.S., Cell spreading and motility: A model lamellipod, *J. Math. Biol.* **21** (1985) 383-388.
- [34] Williams D.R.M. and de Gennes P.G., Cell motility by a non linear osmotic swimming, *Eur. Phys. Lett.* **24** (1993) 311-316.